

## PVT Properties of Pure Lubricants Using Equations of State and Artificial Intelligence

H. Zolfaghari and F. Yousefi\*

*Department of Chemistry, Yasouj University, Yasouj, 75914-353, Iran*

*(Received 3 October 2018, Accepted 31 December 2018)*

In this research, the volumetric properties of lubricants are predicted using two statistical mechanical equations of state called Ihm-Song-Mason and Tao-Mason equations of state at a broad range of temperatures (278.15-398.51 K) and pressures (0.91-600 bar). The equations of state have been examined using corresponding state correlation based on just one input parameter (density at room temperature) as a scaling constant. In addition, the performance of an artificial neural network (ANN) based on back propagation training with 7 neurons in a hidden layer for forecasting the lubricant performance was investigated. The average absolute deviations from literature for 1269 data points of pure lubricants using the improved Ihm-Song-Mason equation of state, Tao-Mason equation of state and ANN at different conditions are calculated to be 0.75%, 0.25% and 0.17%, respectively.

**Keywords:** Lubricant, Statistical mechanics, Artificial neural network, Volumetric property

### INTRODUCTION

Lubricants were introduced to decrease the friction between surfaces in mutual contacts, reducing the heat produced while surface movement. The lubricants may also have the role of transmitting forces, transporting foreign particles, and cooling or heating the surfaces [1]. Additionally, lubricants are used for many other purposes in industrial applications. Other uses include cooking, bio-medical applications on humans, ultrasound test, medical tests, and personal lubricant for sexual purposes.

Recently, a great amount of effort has been made to the extension of procedures for estimating thermophysical properties because the direct measurement of the applicable thermophysical properties over a wide range of temperatures and pressures is unreasonable. The reliable knowledge of the volumetric properties of pure compounds and mixtures is of enormous importance in many fields of research as well as in industrial practice. The densities of fluids as a function of temperature, pressure, and mole

fraction are principally important for the design of industrial plants, pipelines, and pumps. This information is needed for solving material and energy balances required for the design and optimization of chemical processes. Furthermore, reliable density data are the origin for the progress of correlation models and equations of state (EOS).

Equations of state play a central role in modeling thermophysical properties of fluids and if the EOS of a system is established, all thermodynamic behavior of the system can be calculated using the classical thermodynamic relations. The theories of liquids have been expanded based on perturbation theories.

These models have some limitations because of the use of many adjustable parameters or mixing rules requiring an enough data for justification. Therefore, these limitations make them computationally useless. In such cases, an artificial neural network (ANN) can be a proper alternative to model the different thermodynamic properties. The ANN approach is a capable algorithm to approximate certain properties such as density [2]. Yousefi *et al.* used the ANN based on back propagation training with 10 neurons in hidden layer to predict the density of liquid alkali metal

\*Corresponding author. E-mail: [fyousefi@yu.ac.ir](mailto:fyousefi@yu.ac.ir)

alloys in different temperatures and pressures and the obtained results had a good agreement with the experimental data with absolute average deviations of 0.22% [3]. Besides, they applied the ANN with 13 neurons in hidden layer to predict the density of copolymers and the obtained results had a good agreement with the experimental data with absolute average deviations of 0.49% [4]. Zolfaghari *et al.* [5] used Tao-Mason equation of state and the ANN with 19 neurons in hidden layer to predict the behavior of binary mixtures of refrigerant +lubricant fluids and the AADs% of a collection of 3961 data points for all binary mixtures using the EOS and the ANN at various temperatures and mole fractions are 0.92% and 0.34%, respectively.

The Tao-Mason equation of state (TM EOS) [6] has been successfully applied to fluid and their mixtures [7-9]. Moreover, the applications of equation of state and artificial neural networks approaches [10,11] were studied to forecast the properties of pure polymers. This research concentrates on the potential of new version of Ihm-Song-Mason (ISM) EOS, TM EOS and ANN to estimate the volumetric properties of some lubricants in wide range of temperatures and pressures. As a final point, the efficiency of these models is evaluated by the experimental data.

## THEORY

### Equation of State

Statistical mechanics provides us the following equation, assuming a pair-wise additive central intermolecular potential [12],

$$\frac{P}{\rho kT} = 1 - \left(\frac{2\pi\rho}{3kT}\right) \int_0^\infty \left(\frac{\partial u}{\partial r}\right) g(r) r^3 dr \quad (1)$$

where  $[P, \rho, g(r)]$  are the pressure, the density and the pair distribution function. Also,  $(\partial u/\partial r)$  is the derivative of the intermolecular potential  $(u(r))$  with respect to distance  $(r)$ . Ihm *et al.* [13] derived the following equation, applying the Weeks-Chandler-Anderson division for the potential energy function [14],

$$\frac{P}{\rho kT} = 1 + B_2\rho + \alpha\rho[G(b\rho) - 1] \quad (2)$$

where,  $B_2$ ,  $\alpha$ ,  $G(b\rho)$  and  $b$  are the second virial coefficient, the repulsive contribution to the second virial coefficient, the average pair distribution function at contact for equivalent hard spheres and the analog of the van der Waals covolume.

$$b = \alpha + T \frac{d\alpha}{dT} \quad (3)$$

Each of the temperature-dependent parameters ( $B_2$ ,  $\alpha$  and  $b$ ) can be written in terms of the intermolecular pair potential as [15],

$$B_2 = 2\pi \int_0^\infty [1 - \exp(-\frac{u}{kT})] r^2 dr \quad (4)$$

$$\alpha = 2\pi \int_0^{r_m} [1 - \exp(-\frac{u_0}{kT})] r^2 dr \quad (5)$$

and

$$b = \frac{2}{3} \pi d^3 = 2\pi \int_0^{r_m} [1 - (1 + \frac{u_0}{kT}) \exp(-\frac{u_0}{kT})] r^2 dr \quad (6)$$

where  $d$  and  $u_0$  are the effective hard-sphere diameter and the repulsive branch of intermolecular pair potential.

Ihm *et al.* [13] performed a correction in Eq. (2) for the attractive forces using the Carnahan-Starling equation for  $G(b\rho)$  [16],

$$\frac{P}{\rho kT} = 1 - \frac{(\alpha - B_2)\rho}{1 + 0.22\lambda b\rho} + \frac{\alpha\rho}{1 - \lambda b\rho} \quad (7)$$

where  $\lambda$  is an adjustable parameter obtained from some experimental P-V-T data at high density.

Tao and Mason added a perturbation modification term which affects the attractive forces to ISM equation of state [13] to present an advanced equation of state [17]. The TM EOS [17] for pure system is as follows:

$$\frac{P}{\rho kT} = 1 + (B_2 - \alpha)\rho + \frac{\alpha\rho}{1 - \lambda b\rho} + A_1(\alpha - B)b\rho^2 \frac{(e^{\frac{\kappa T_c}{T}} - A_2)}{1 + 1.8(b\rho)^4} \quad (8)$$

where

$$A_1 = 0.143$$

$$A_2 = 1.64 + 2.65[e^{(\kappa-1.093)} - 1] \quad (9)$$

$$\kappa = 1.093 + 0.26 \left[ (\omega + 0.002)^{\frac{1}{2}} + 4.50(\omega + 0.002) \right] \quad (10)$$

$\omega$ ,  $\lambda$  and  $\rho$  are the Pitzer acentric factor, adjustable parameter and the number density, respectively.  $T_C$ ,  $B_2$ ,  $\alpha$  and  $b$  are the critical temperature, the second virial coefficient, the scaling parameter and the effective van der Waals co-volume, respectively.

The second virial coefficient,  $B_2$ , along with the parameters  $\alpha$ , and  $b$  are required to use TM EOS. It should be stated that if the intermolecular potential is not available, the knowledge of experimental second virial coefficient data is sufficient to calculate values of  $\alpha$  and  $b$  parameters [6]. In this case, there are several correlations to calculate the second virial coefficient.

The Tsonopolous correlation to calculate the  $B_2$  values is presented as follows [18]:

$$B_2\left(\frac{P_C}{RT_C}\right) = f^{(0)}(T_r) + \omega f^{(1)}(T_r) \quad (11)$$

where  $T_r$  is reduced temperature.

$$f^{(0)}(T_r) = 0.1445 - \frac{0.330}{T_r} - \frac{0.1385}{T_r^2} - \frac{0.0121}{T_r^3} \quad (12)$$

$$f^{(1)}(T_r) = 0.0637 + \frac{0.331}{T_r^2} - \frac{0.423}{T_r^3} - \frac{0.008}{T_r^8} \quad (13)$$

To achieve the higher accuracy, a corresponding state correlation was investigated to make ISM and TM EOS applicable in pure lubricants. In this respect, the following correlation equation for  $B_2$  using new scaling parameter (molar density at the room temperature) has been developed,

$$B_2\rho_r = [1.033 - 3.0069\left(\frac{298.15}{T}\right) - 10.588\left(\frac{298.15}{T}\right)^2 + 13.096\left(\frac{298.15}{T}\right)^3 - 9.8968\left(\frac{298.15}{T}\right)^4] \quad (14)$$

where  $\rho_r$  is molar density at room temperature.

The empirical equations given in Ref. [6] for  $a/v_B$  and  $b/v_B$  as a function of  $T/T_B$  can be rescaled by  $T_r$  (298.15) and  $\rho_r$  (room temperature and density) instead of  $T_B$  and  $v_B$  as pointed out by Eslami [19],

$$\alpha\rho_r = a_1 e^{-c_1 T_m} + a_2 \left[ 1 - e^{-c_2/T_m^{1/4}} \right] \quad (15)$$

$$b\rho_{bp} = a_1 \left[ 1 - c_1 T_m \right] e^{-c_1 T_m} + a_2 \left\{ 1 - \left[ 1 + \frac{c_2}{4T_m^{1/4}} \right] e^{\frac{-c_2}{T_m^{1/4}}} \right\} \quad (16)$$

where  $T_m = T/298.15$ , and the constants  $a_1$ ,  $a_2$ ,  $c_1$ ,  $c_2$  are -0.0860, 2.3988, 0.5624, 1.4267, respectively. All equations are coded in MATLAB software.

### Artificial Neural Network (ANN) Modeling

An ANN is a non-linear mathematical method which is notable because of its simplicity, flexibility, and accessibility [20-22]. The ANN is obtained based on the activity of human brain and has been applied to many scientific models [21-24]. Various applications and details of the ANN were presented in prior publications [25,26].

An ANN is formed by the input layer, the output layer, and one or more neuron layers (named hidden layers), which can be laid between them (Fig. 1). Figure 1 shows the schematic presentation of the ANN model. The construction of the ANN is identified using the number of network layers, the number of neurons in each layer, the nature of learning algorithms and the neuron transfer functions.

### Network Training and Choice of the Top Topology of Network

One kind of feed forward neural network that has been used commonly for the approximate function is multilayer perceptron (MLP). They adjust weights of the neurons with the difference between the values of actual and target output. This technique offers a non-linear regression between input and output variables and is very expensive in

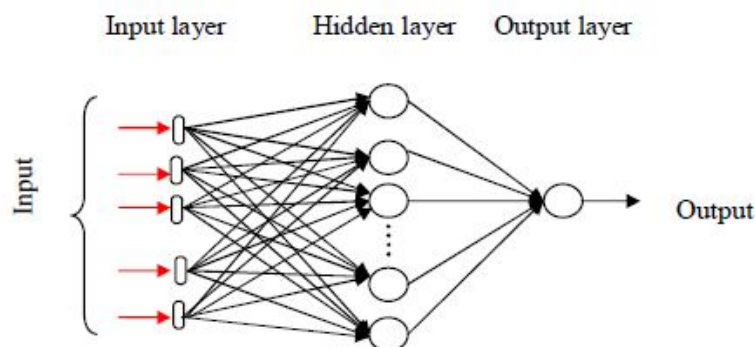


Fig. 1. The MLP structure.

identifying patterns in complex data. The back-propagation algorithm is one of the most important training algorithms. Two common transfer functions that are used in the hidden layer and output layer are “Tansig” and “Purelin”. Furthermore, the best network organization is explained via the back propagation algorithm of Levenberg–Marquardt (trainlm).

The mathematical definition of the errors criteria including mean square error (MSE), absolute average deviation percentage (AAD%) and coefficient of determination ( $R^2$ ) were defined as below:

$$MSE = \sum_{i=1}^N (\rho_i^{\text{exp}} - \rho_i^{\text{cal}})^2 \quad (17)$$

$$AAD(\%) = \frac{1}{N} \sum_{i=1}^N \left( \left| \frac{\rho_i^{\text{exp}} - \rho_i^{\text{cal}}}{\rho_i^{\text{exp}}} \right| \right) \times 100 \quad (18)$$

$$R^2 = \frac{\sum_{i=1}^N (\rho_i^{\text{exp}} - \bar{\rho})^2 - \sum_{i=1}^N (\rho_i^{\text{exp}} - \rho_i^{\text{cal}})^2}{\sum_{i=1}^N (\rho_i^{\text{exp}} - \bar{\rho})^2} \quad (19)$$

where  $N$ ,  $\rho_i^{\text{exp}}$  and  $\rho_i^{\text{cal}}$  are number of data, experimental and calculated density, respectively.

The neural network programming was provided in ANN tool box of MATLAB software.

## RESULTS AND DISCUSSION

In this study, the PVT properties of lubricant are obtained from the extended SM and TM EOS. Subsequently, the artificial intelligence model was trained

over the complete range of temperatures and pressures. The experimental data were taken from ref. [27-38] and all of them are used for modeling and comparison.

Some changes are applied to extend the original ISM and TM EOS as follows: 1) the second virial coefficient was improved using the density at room temperature (that simply can be calculated against the critical parameters). 2) The number of input parameters in the Tsonopolous' correlation [18] is reduced to just one parameter ( $\rho_r$ ) by the Eslami correlation [19]. 3)  $k$  in Eq. (10) is a weak function of the acentric factor so that  $k$  is estimated to be 1.093 and  $A_2$  was changed to 1.64.4)  $\alpha$  and  $b$  were formulated using Eqs. (15) and (16), respectively. In both equations, the input parameters (the molar density at room temperature) are more available than the Boyle temperature and volume. Overall, the number of input parameters is reduced from five (critical temperature, critical pressure, acentric factor, Boyle temperature, and Boyle volume) to just one (molar density at room temperature).

In this work,  $\lambda$  for pure lubricants was adjusted by a nonlinear regression technique as follow:

$$\lambda = a + bT + cP + dT^2 + eP^2 + fTP + dT^3 \quad (20)$$

The abbreviation and physical properties of all pure lubricants are present in Table 1 and the required parameters to calculate of  $\lambda$  for pure lubricants are listed in Table 2.

In this project, to predict the PVT properties of lubricants, the temperature ( $T$ ), pressure ( $P$ ), molecular weight and normal boiling temperature of pure lubricant are

**Table 1.** Abbreviation and Physical Properties of Pure Lubricant

Full name of lubricant	Abbreviation	M <sub>w</sub> (g mol <sup>-1</sup> )	ρ <sub>r</sub> (Kg m <sup>-3</sup> )	T <sub>b</sub> (K)
Tetraethylene glycol dimethyl ether	TEGDME	222.28	1009	548.15
Dimethyl carbonate	DMC	178.23	986	489.15
Triethylene glycol dimethyl ether	TriEGDME	416.51	1070	752.45
Pentaerythritol ester of butyric acid	PEC4	472.62	1038	801.45
Pentaerythritol tetrapentanoate	PEC5	528.73	1014	847.55
Pentaerythritol ester of hexanoic acid	PEC6	584.82	995	891.15
Pentaerythritol tetraheptanoate	PEC7	640.94	981	932.65
Pentaerythritol ester of octanoic acid	PEC8	697.04	969	972.25
Pentaerythritol tetranonanoate	PEC9	640.94	978	920.85
Pentaerythritol tetra(2-ethylhexanoate)	PEB8	90.08	1073	363.15
2,6,10,15,19,23-Hexamethyltetracosane	Squalane	422.81	804.9	743.45
Diethylene glycol monoethyl ether	DEGEE	134.17	999	475.15

**Table 2.** Coefficients in Eq. (21)

Lubricant	a	b	c	d × 10 <sup>-7</sup>	e	F × 10 <sup>-7</sup>
TEGDME	0.4767	7.5871 × 10 <sup>-5</sup>	-0.00017	-6.076	-7.2260 × 10 <sup>-8</sup>	8.148
TriEGDME	0.4784	6.5868 × 10 <sup>-5</sup>	-0.00016	-5.768	-5.4012 × 10 <sup>-8</sup>	7.179
PEC4	0.5038	-4.058010 <sup>-6</sup>	-0.00029	-5.456	-2.042510 <sup>-7</sup>	15.05
PEC5	0.5028	-2.7479 × 10 <sup>-5</sup>	-0.00024	-4.758	-2.068 × 10 <sup>-7</sup>	13.867
PEC6	0.5098	-5.7283 × 10 <sup>-5</sup>	-0.00031	-4.401	-3.0462 × 10 <sup>-7</sup>	17.52
PEC7	0.5034	-6.1586 × 10 <sup>-5</sup>	-0.00023	-3.879	-2.709 × 10 <sup>-7</sup>	15.013
PEC8	0.5099	-7.0716 × 10 <sup>-5</sup>	-0.00030	-3.909	-3.8952 × 10 <sup>-7</sup>	18.87
PEC9	0.5102	-0.00012	-0.00022	-2.660	-3.484 × 10 <sup>-7</sup>	15.980
PEB8	0.5167	-0.0001	-0.00022	-2.843	-3.5756 × 10 <sup>-7</sup>	15.45
DMC	0.4055	0.0005	-0.00010	-10.54	-8.3954 × 10 <sup>-9</sup>	3.463
Squalane	0.4917	-5.8360 × 10 <sup>-5</sup>	-0.00018	-3.493	-2.2522 × 10 <sup>-7</sup>	12.50
DEGEE	0.4584	0.0003	-0.00020	-10.10	-4.6055 × 10 <sup>-8</sup>	8.059

**Table 3.** Summary of the Input-output Dataset Characterization

Lubricant	NP	$\Delta T$ (K)	$\Delta P$ (bar)	Tb (K)	$\Delta \rho$ (g cm <sup>-3</sup> )	Ref.
TEGDME	204	278.15-373.15	1-600	548.15	0.9375-1.0515	[29,30]
TriEGDME	204	278.15-373.15	1-600	489.15	0.9086-1.0275	[31]
PEC4	40	283.15-343.15	1.04-348.48	752.45	1.008-1.0782	[32]
PEC5	99	278.15-353.15	1-450	801.45	0.9744-1.0586	[33]
PEC6	40	283.15-343.15	0.91-344.34	847.55	0.9573-1.0222	[32]
PEC7	99	278.15-353.15	1-450	891.15	0.9391-1.0186	[34]
PEC8	40	283.15-343.15	1.05-344.74	932.65	0.9262-0.9885	[32]
PEC9	88	283.15-353.15	1-450	972.25	0.9176-0.9903	[34]
PEB8	99	278.15-353.15	1-450	920.85	0.9195-0.9955	[35]
DMC	141	278.15-353.15	1-400	363.15	0.9883-1.1132	[36,37]
Squalane	143	278.15-398.15	1-600	743.45	0.7421-0.8399	[38,39]
DEGEE	72	283.15-353.15	1-250	475.15	0.9341-1.0113	[40]

used as input variables and the molar densities of lubricants are used as targets. The ranges of input-output variables for each system are given in Table 3. In this table, the number of data points are defined as NP. The experimental data for each lubricant are taken from ref. column.

All experimental data points that used in this study is 1269. The MLP is trained, validated, and tested with a random 70% (889 data points), 15% (190 data points), and 15% (190 data points), respectively.

One of the important problems in the ANN is over-training. It can be overcome through proper choice of the number of neurons in the hidden layer (Fig. 2). Training step should increase with increasing hidden neuron number, and an optimal number of hidden neurons leads to the best performance of the network in testing data phase. This trained network yields the best prediction on testing data and the use of more or less than the optimal number of hidden neurons was discouraged. The mean square error (MSE), average absolute deviation (AAD%) and correlation

coefficient ( $R^2$ ) of training and testing data were selected as a measure of the performance of the net. As a result, the network with one hidden layer (7 neurons) with grateful values of MSE, AAD and  $R^2$  of training and testing data (Table 4), produced the best prediction. Figure 3 shows the training, validation, and test deviations as a function of the number of training epochs (based on early stopping approach). The training stopped when the network converged. In this situation, the mean squared error is relatively constant over 37 iterations. It should be stated that, the neural network with the randomly assigned initial weights and biases cannot accurately estimate the required output. Therefore, the weights and biases are modified by the training to minimize the difference between the model output and target (observed) values (Table 5). Table 5 presents all optimal calculated weights and biases of trained network.

The best neural network model was utilized to predict the PVT properties of lubricants based on training and

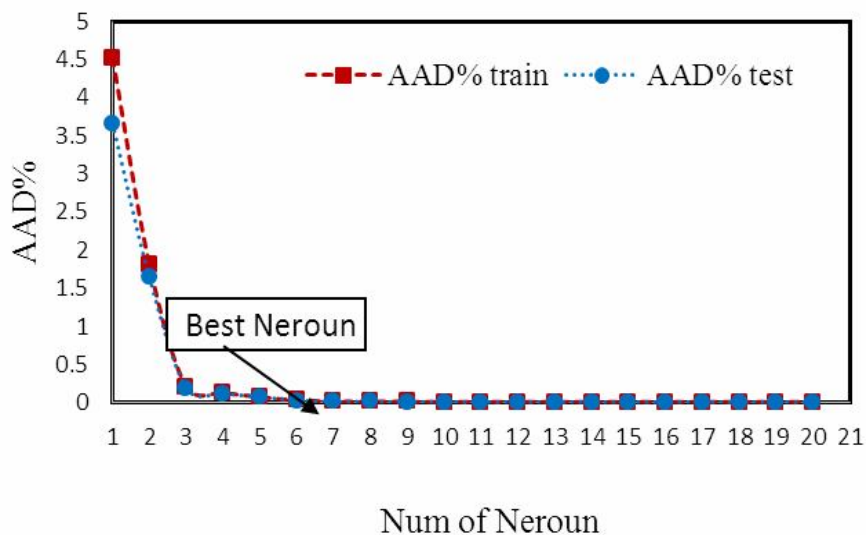


**Fig. 2.** Effect of the number of hidden layer neurons on AAD%.

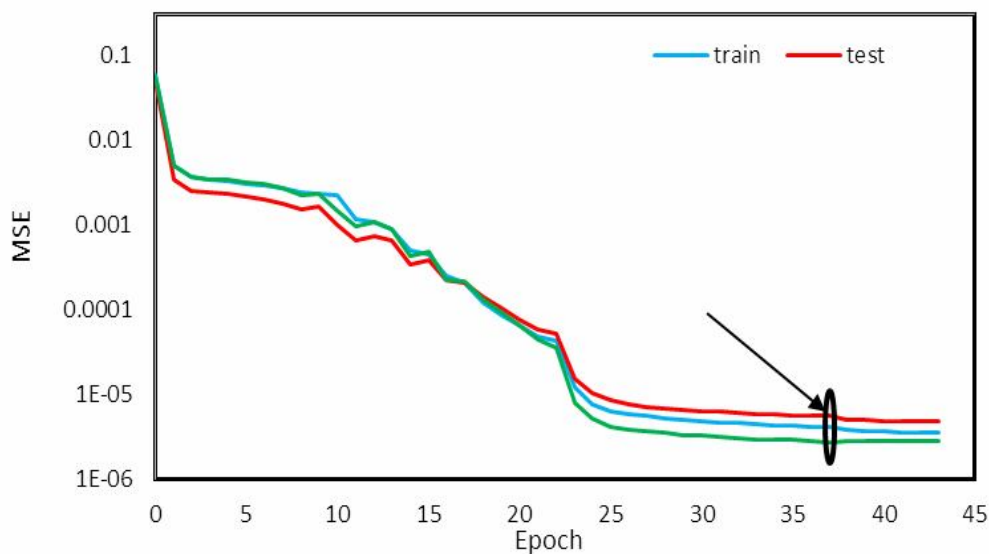


**Fig. 3.** Evolution of training, validation, and test errors as a function of the number of training epochs during ANN training.

testing data. The comparison of the predicted and experimental values of training and testing data are shown in Figs. 4a and 4b. These figures demonstrate that there is good harmony between the predicted and the experimental values of training and testing data of lubricants with average absolute deviations of 0.0154% and 0.0156% and high

correlation coefficients, 1.0000 and 1.0000, respectively. In addition, the error analysis of training, testing and validation data by temperature variation are presented in Fig. 5. This figure illustrates that the minimum, maximum, and mean standard deviations for predicting the neural network are 0.0003, 0.5863 and 0.1700, respectively.

**Table 4.** The Results of AAD%, MSE and R<sup>2</sup> to Optimize the Number of Neuron in Hidden Layer

Net	Training			Testing		
	AAD%	MSE	R <sup>2</sup>	AAD%	MSE	R <sup>2</sup>
1	4.5270	3.54E-03	0.55798	3.6667	2.66E-03	0.59814
2	1.8119	4.74E-04	0.95318	1.6440	4.11E-04	0.95419
3	0.2091	7.37E-06	0.99925	0.1924	6.75E-06	0.99934
4	0.1298	2.77E-06	0.99974	0.1215	2.40E-06	0.99971
5	0.0757	2.21E-06	0.99978	0.0771	2.39E-06	0.99980
6	0.0320	1.55E-07	0.99998	0.0307	1.42E-07	0.99999
7	0.0154	4.41E-08	1.00000	0.0156	4.60E-08	1.00000
8	0.0145	3.47E-08	1.00000	0.0143	3.50E-08	1.00000
9	0.0130	2.83E-08	1.00000	0.0124	2.49E-08	1.00000
10	0.0121	2.47E-08	1.00000	0.0120	2.31E-08	1.00000
11	0.0115	2.26E-08	1.00000	0.0106	1.95E-08	1.00000
12	0.0112	2.27E-08	1.00000	0.0103	1.70E-08	1.00000
13	0.0112	2.15E-08	1.00000	0.0101	1.64E-08	1.00000
14	0.0105	1.92E-08	1.00000	0.0094	1.45E-08	1.00000
15	0.0099	1.90E-08	1.00000	0.0092	1.33E-08	1.00000
16	0.0093	1.68E-08	1.00000	0.0095	1.61E-08	1.00000
17	0.0096	1.83E-08	1.00000	0.0094	1.76E-08	1.00000
18	0.0094	1.64E-08	1.00000	0.0085	1.17E-08	1.00000
19	0.0086	1.44E-08	1.00000	0.0082	1.26E-08	1.00000
20	0.0085	1.54E-08	1.00000	0.0088	1.75E-08	1.00000

The densities of lubricants based on the TM EOS under various conditions were computed and compared with experimental data [27-38].

Finally, the ANN, ISM and TM EOS were evaluated with literature values [27-38] for all lubricants. The TM EOS and ANN have good harmony with experimental data. Therefore, all figures present the AAD% plot of two excellent models with experiment.

The computed molar densities of DEGEE from TM

EOS and ANN at different temperatures and pressures are compared with experimental data [38] and the deviation plot of this system versus pressure at different temperatures is shown in Fig. 6. This figure presents a good agreement between the TM EOS and ANN with the literature with the overall average absolute deviations of 0.034 and 0.075 from the literature data, respectively.

The average absolute deviations from experimental data [34,35] for the predicted molar densities of the dimethyl

**Table 5.** The Optimal Weights and Biases for Hidden and Output Layers of ANN

Hidden layer connectivity							
Wij					Bi		
-0.07321	-0.29988	0.14014	-1.64004	1.62087	-0.07321		
3.56231	0.14145	-0.03541	-0.79087	3.95784	3.56231		
0.43081	-0.10014	0.01125	-5.11718	-1.57500	0.43081		
0.58875	1.14282	1.33406	-0.96857	-1.162046	0.58875		
1.89764	-0.09617	0.00930	0.09048	-8.44102	1.89764		
1.40587	1.14769	0.06322	-0.54521	2.54325	1.40587		
-2.38583	-0.07287	-0.04041	-2.48346	-1.17697	-2.38583		
Output layer connectivity							
Wji							bi
0.74626	-1.24307	4.41939	-0.00640	-4.35258	-0.072021	-0.28749	1.25419

i: representative of neuron; j: representative of corresponding inputs.

Carbonate are calculated from the improved TM EOS and ANN and the overall AAD% are 0.03% and 0.12%, respectively (see Fig. 7). The improved TM EOS is better than the artificial intelligent.

The TM EOS and the ANN were performed to calculate the densities of PEB8 and plot the deviation of this system from experiment [33] *versus* pressure at various temperatures as presented in Fig. 8. The overall AAD% of TM EOS and ANN are 0.76% and 0.11%, respectively. The ANN is superior to the new equation of state.

Densities of PEC4 calculated from the new TM equation of state and ANN at various temperatures and pressures and AAD% plot of this lubricant from experimental data [30] are presented in Fig. 9. The overall AAD% of TM EOS and ANN are 0.14% and 0.04%, respectively. The ANN is superior to the new equation of state.

The average absolute deviations from experimental data [31] for the predicted densities of the PEC5 are calculated from EOS and ANN, and the deviation plot *via* pressure at different temperatures is shown in Fig. 10. The AAD% of TM EOS and ANN are 0.27% and 0.07%, respectively.

The calculated molar densities of PEC6 in various

temperatures and pressures are performed and the AAD% from experimental data [30] is presented in Fig. 11. This figure shows that the AAD% of TM EOS and ANN for 40 data points are 0.196% and 0.104%, respectively.

The calculated molar densities of PEC7 in temperature range of 278.15-353.15 K and pressure range of 1-450 bar are performed and the AAD% from experimental data [32] is presented in Fig. 12. The AAD% of TM EOS and ANN for 99 data points are 0.350% and 0.099%, respectively.

The average absolute deviations from experimental data [30] for the predicted densities of the PEC8 in temperature range of 283.15-343.15 K and pressure range of 1.05-344.74 bar are calculated from TM EOS and ANN and the deviation plot *via* pressure at different temperatures is shown in Fig. 13. The AAD% of TM EOS and ANN for 40 data points are 0.261% and 0.916%, respectively.

Densities of PEC9 calculated from the new TM equation of state and ANN at various temperatures and pressures and AAD% plot of this lubricant from experimental data [32] is presented in Fig. 14. The overall AAD% of TM EOS and ANN for 88 data points are 0.421% and 0.185%, respectively. The ANN is superior to the new equation of

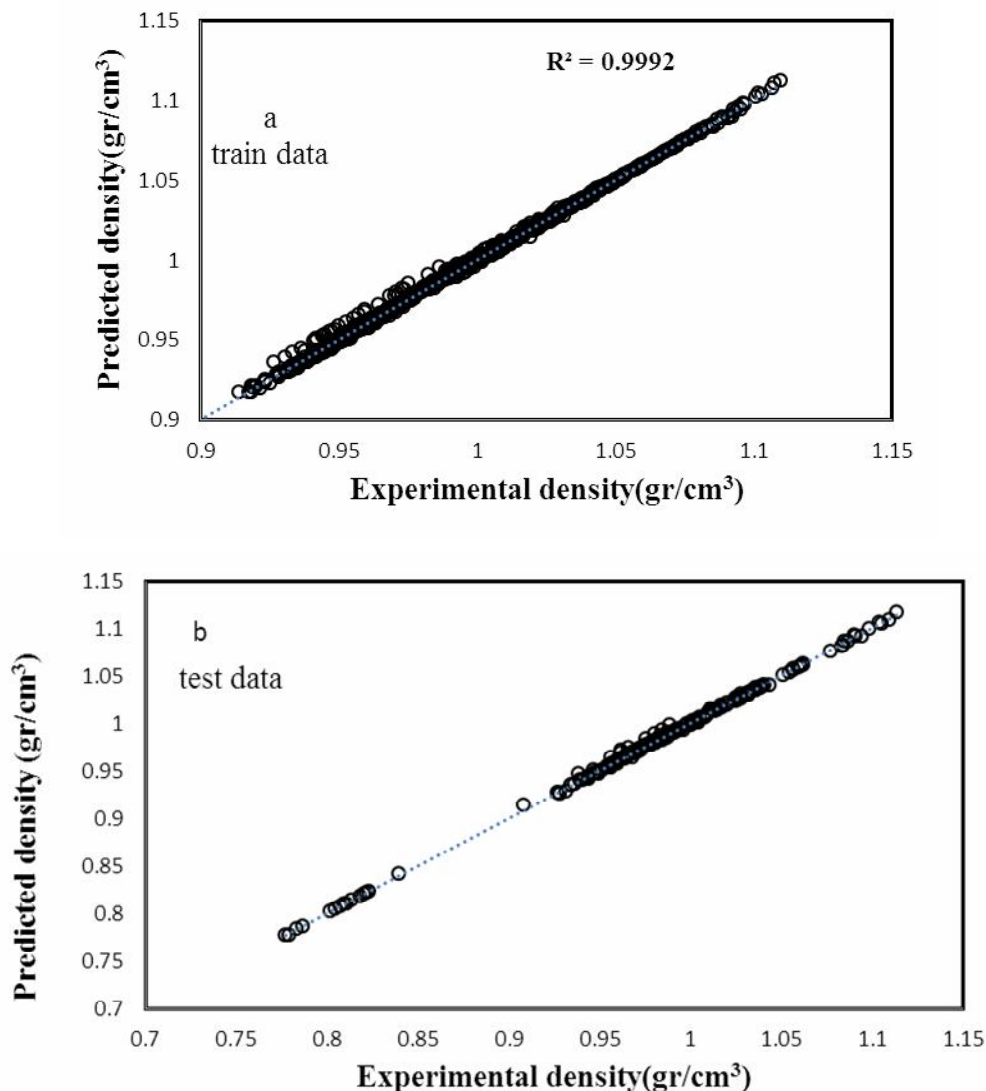


**Fig. 4.** Modeling ability of the optimized ANN to predict the densities of all pure lubricants (a) for training data (b) for testing data.

state.

The calculated molar densities of Squalance, TEGDME and Tri EDME, in various temperatures and pressures are performed and the AAD% from experimental data [27-29,36,37] are presented in Figs. 15-17. These figures show that the ANN is better than the new version of TM EOS but both of methods have good agreement with experimental data. It should be stated that although the error of obtained result from artificial neural network with the literature is smaller than that from EOS but the equation of state based

on the statistical mechanics is very important in thermodynamic science. Because of all behavior of molecules (such as interaction of molecules) are defined in equation of state based on statistical mechanics while the artificial neural network is a black box.

Furthermore, in this work, ISM EOS is extended by the above mentioned corrections and the results are compared with those obtained using TM EOS and ANN. The AAD% of the calculated molar densities of pure lubricants using the improved ISM EOS, TM EOS and ANN at different

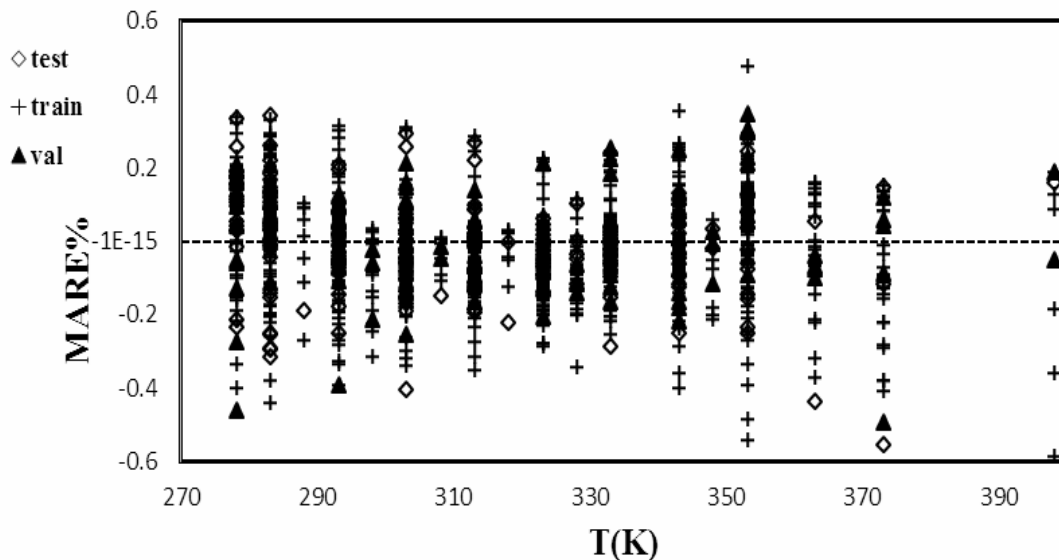


Fig. 5. Mean absolute relative error for the train, test and validation density of all pure lubricants with the experimental data.

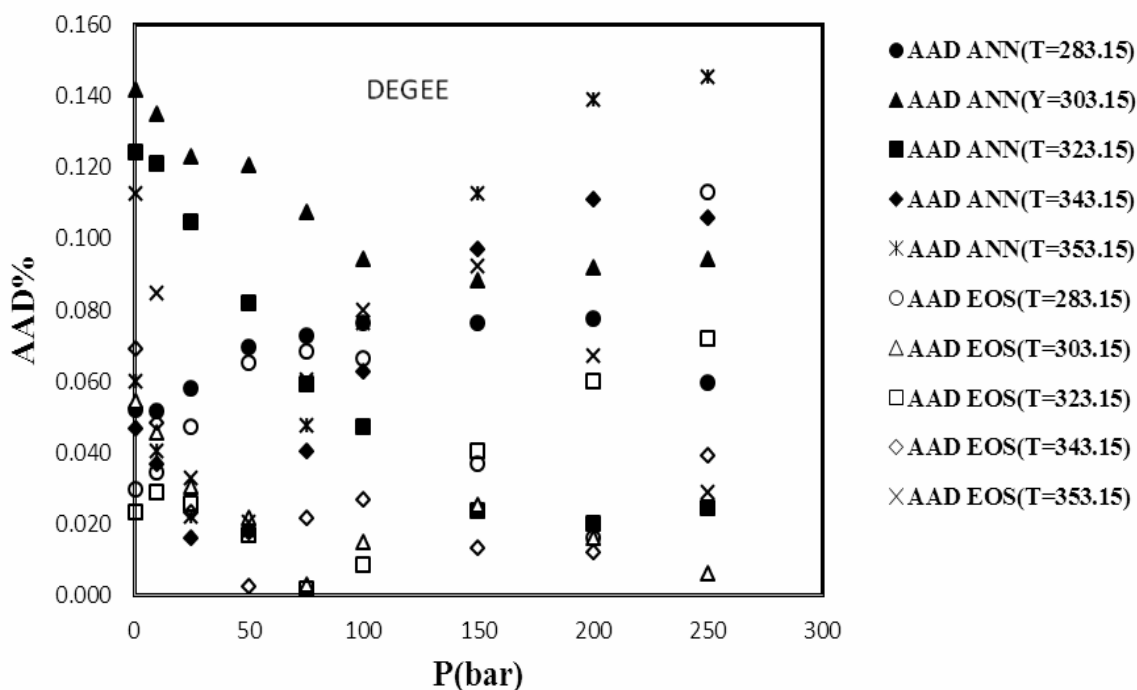


Fig. 6. The deviation plot of the calculated density vs. pressure for DEGEF in different temperatures, using TM EOS and ANN from the literature data [40].

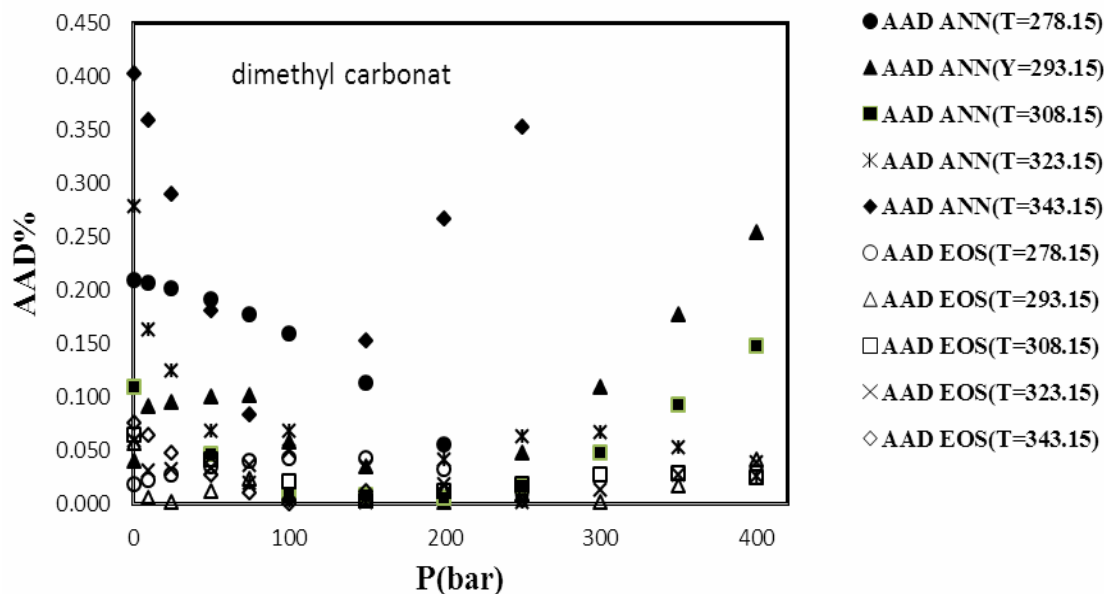


Fig. 7. The deviation plot of the calculated density vs. pressure for Dimethyl Carbonate in different temperatures, using TM EOS and ANN from the literature data [36,37].

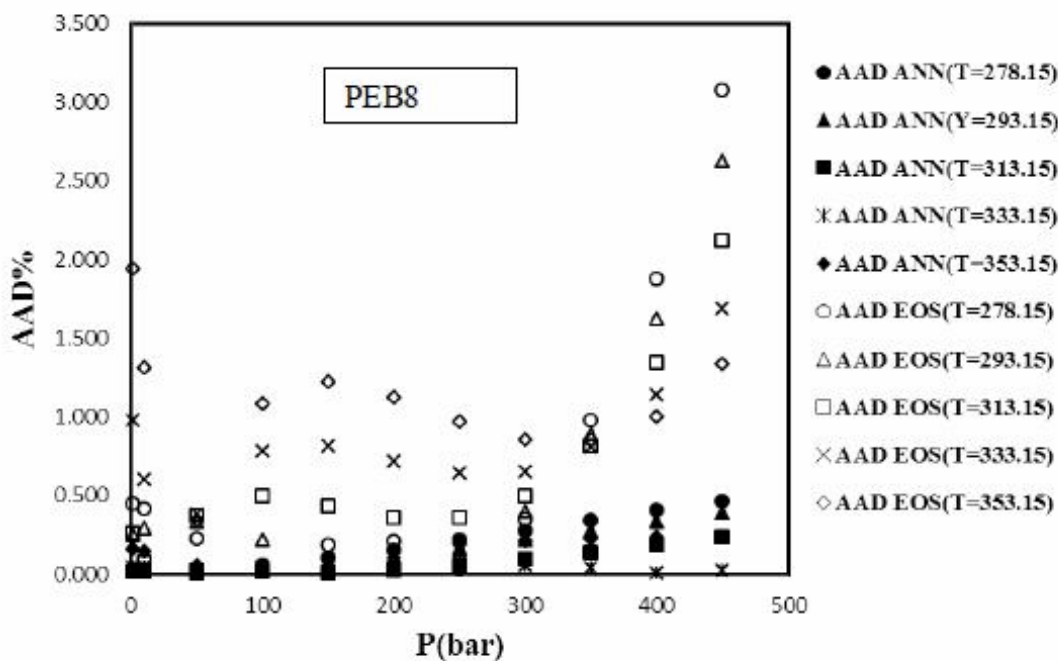
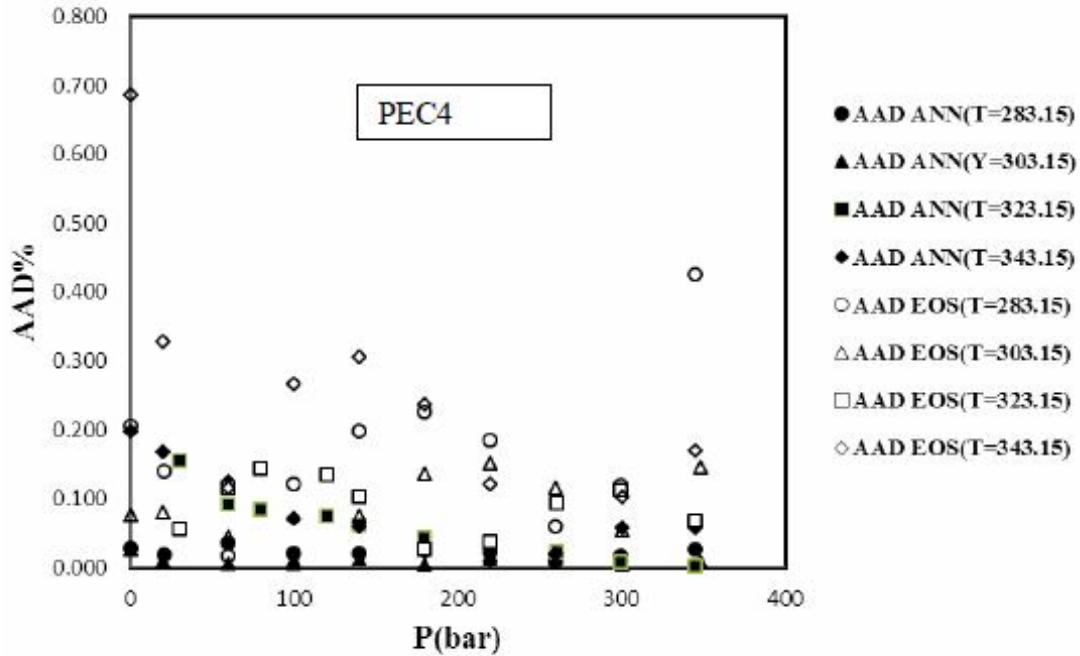
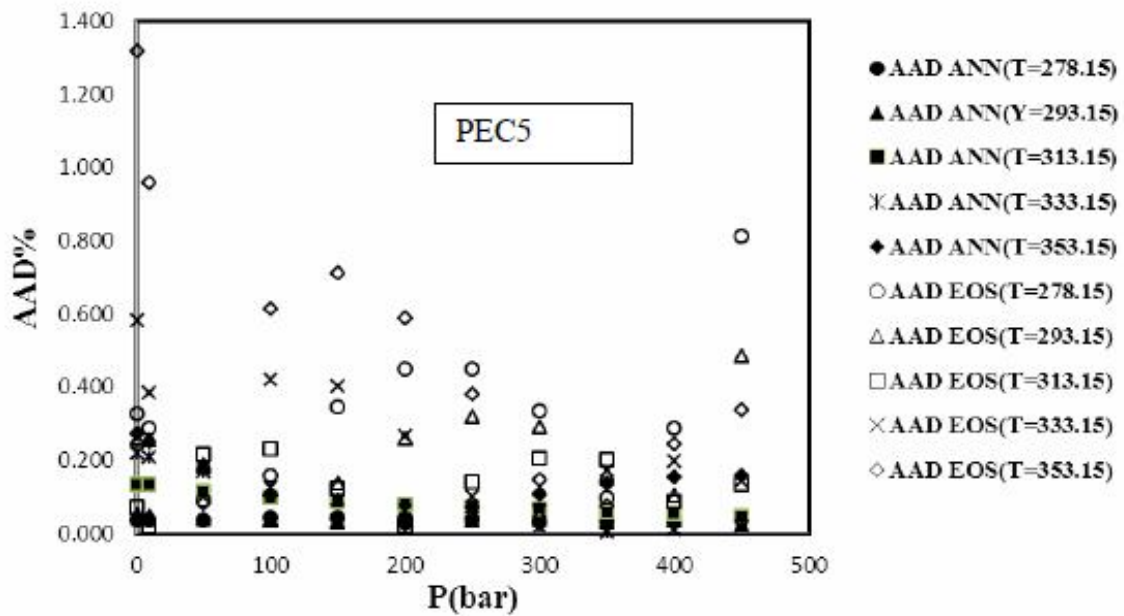


Fig. 8. The deviation plot of the calculated density vs. pressure for PEB8 in different temperatures, using TM EOS and ANN from the literature data [35].



**Fig. 9.** The deviation plot of the calculated density vs. pressure for PEC4 in different temperatures using TM EOS and ANN from the literature data [32].



**Fig. 10.** The deviation plot of the calculated density vs. pressure for PEC5 in different temperatures, using TM EOS and ANN from the literature data [33].

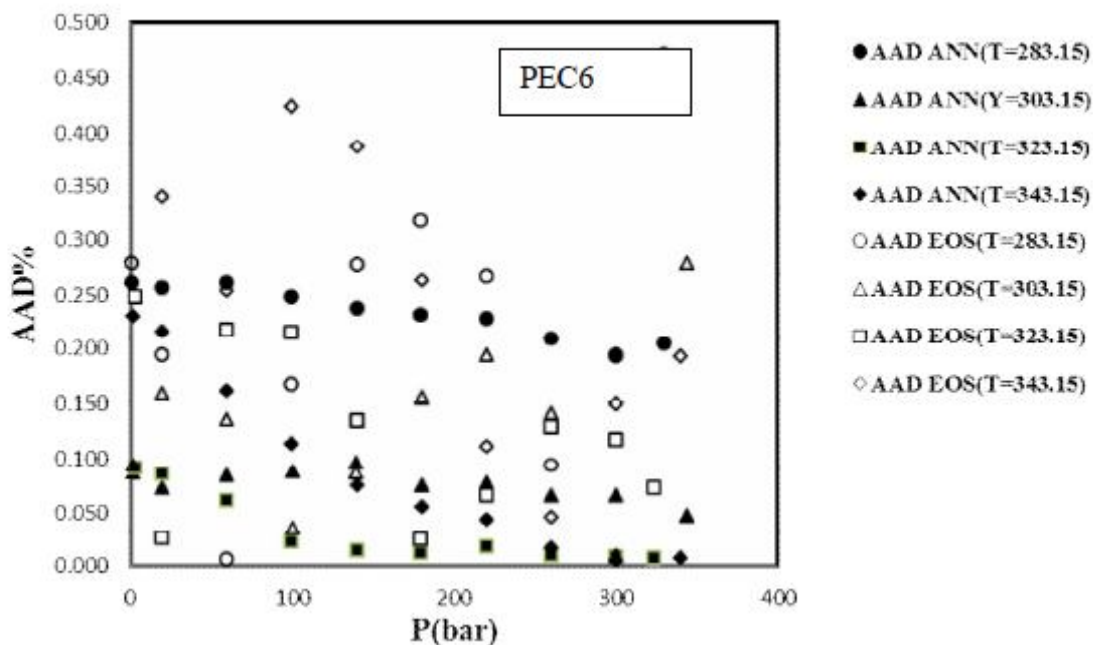


Fig. 11. The deviation plot of the calculated density vs. pressure for PEC6 in different temperatures, using TM EOS and ANN from the literature data [32].

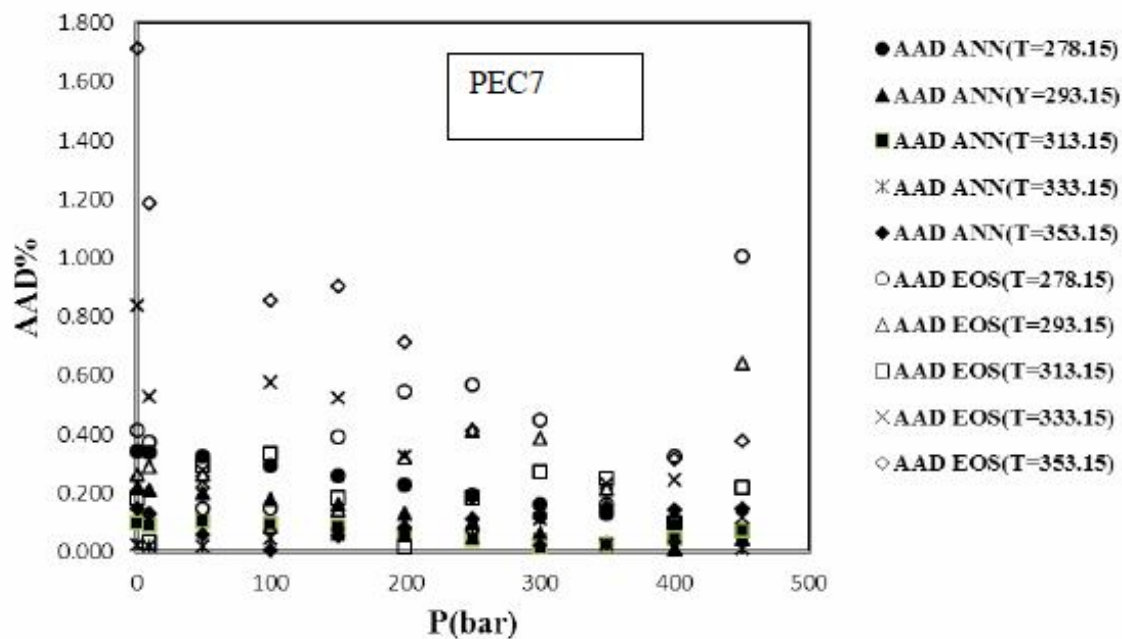


Fig. 12. The deviation plot of the calculated density vs. pressure for PEC7 in different temperatures, using TM EOS and ANN from the literature data [33].

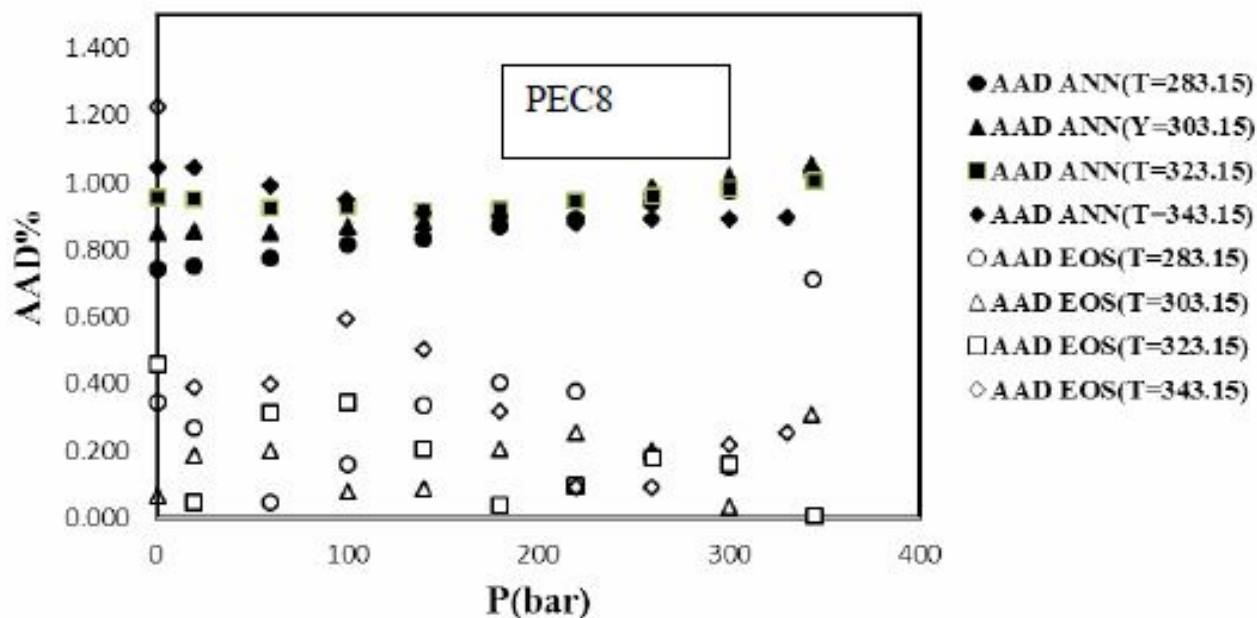


Fig. 13. The deviation plot of the calculated density vs. pressure for PEC8 in different temperatures, using TM EOS and ANN from the literature data [32].

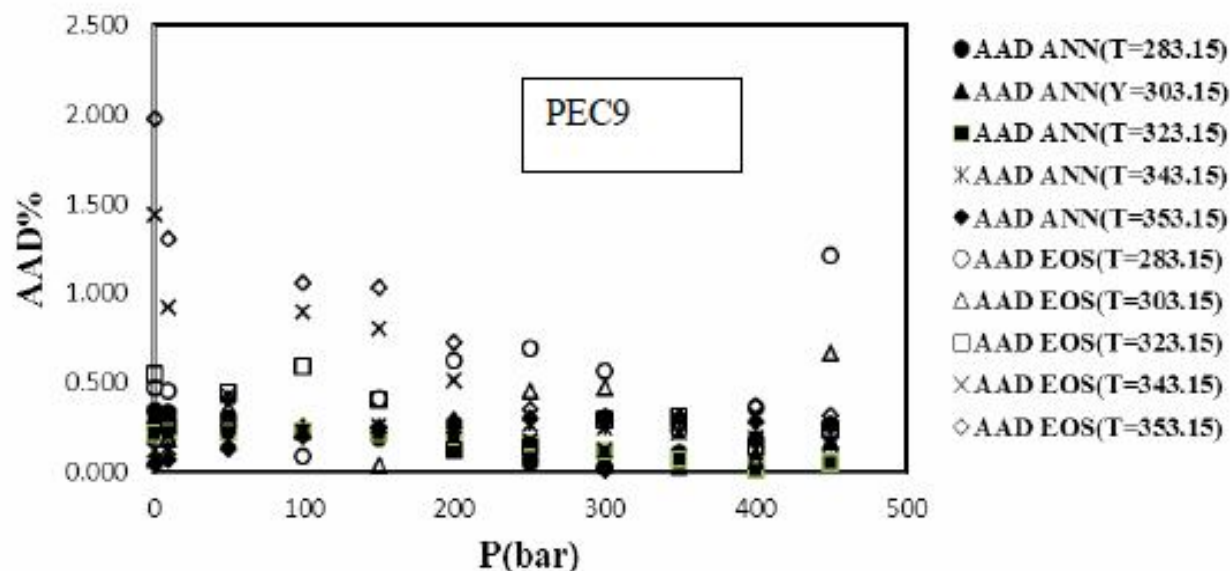


Fig. 14. The deviation plot of the calculated density vs. pressure for PEC9 in different temperatures, using TM EOS and ANN from the literature data [33].

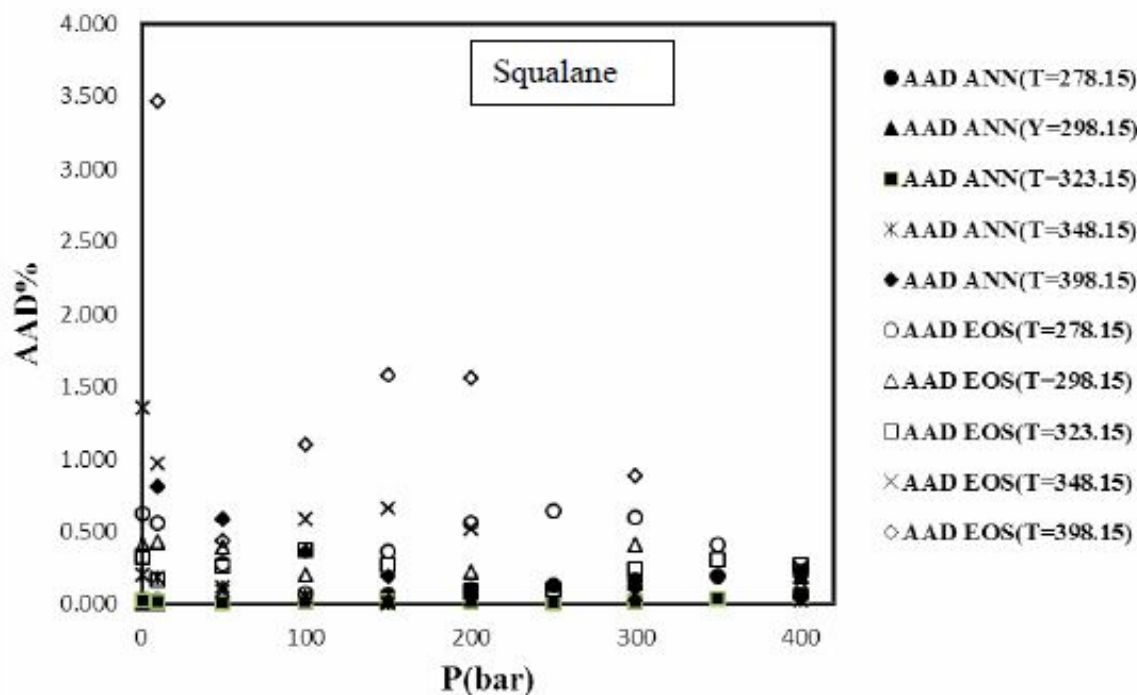


Fig. 15. The deviation plot of the calculated density vs. pressure for Squalane in different temperatures, using TM EOS and ANN from the literature data [38,39].

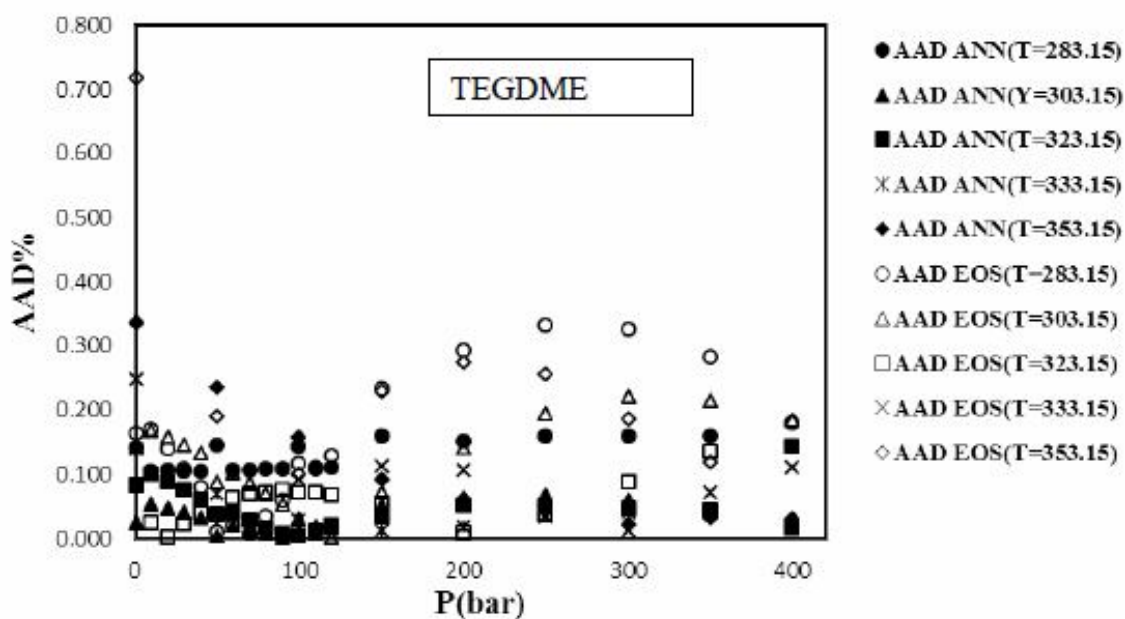


Fig. 16. The deviation plot of the calculated density vs. pressure for TEGDME in different temperatures, using TM EOS and ANN from the literature data [29,30].

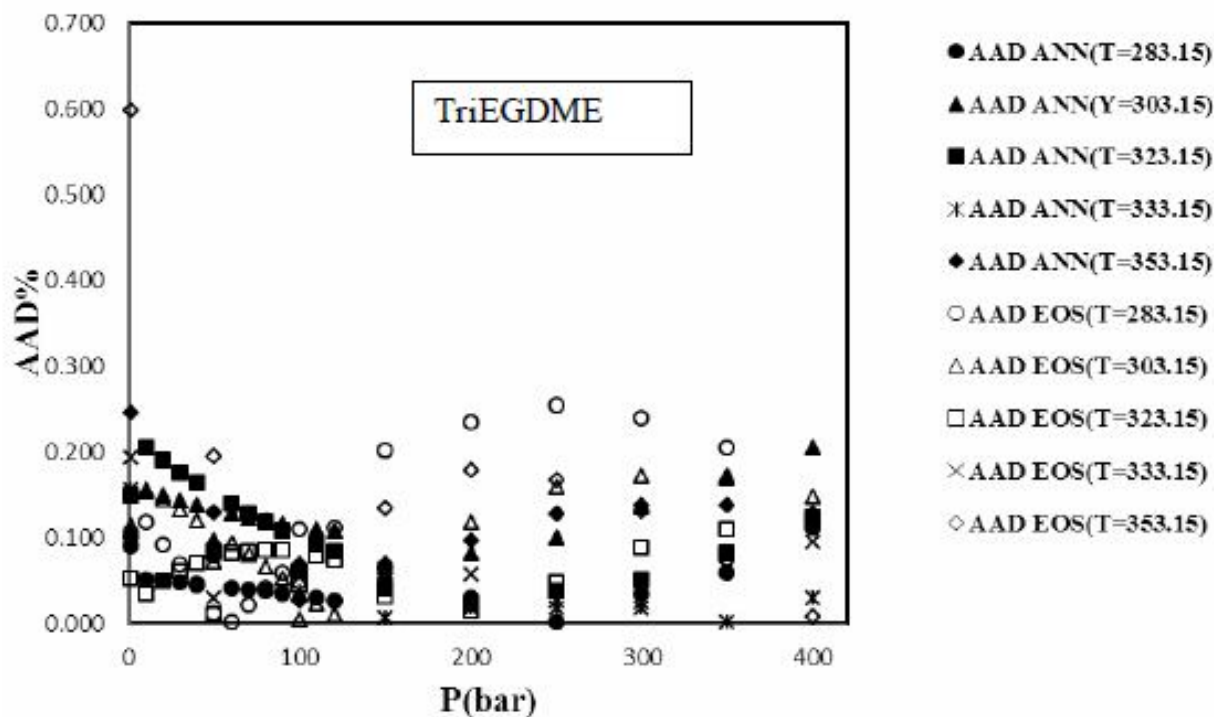


Fig. 17. The deviation plot of the calculated density vs. pressure for Tri EDME in different temperatures, using TM EOS and ANN from the literature data [31].

temperatures and pressures are collected in Table 6. Besides, this table includes the number of data point (NP), pressure, and temperature ranges of all studied pure lubricants. The overall average absolute deviation of ISM EOS, TM EOS and ANN for 1269 data points are 0.75%, 0.25% and 0.17%, respectively.

#### \*NP is Nnumber of Data Points

Generally, the other important characteristic of the ISM and TM EOS are predicting of PVT properties of pure lubricants with minimum available input information; there is no need to specify the potential energy curve, the experimental second virial coefficients, the critical constant, or some parameters like the Pitzer acentric factor and the heat of vaporization.

## CONCLUSIONS

The ISM and TM EOS based on statistical mechanics

and artificial neural networks models are developed to predict the volumetric properties of pure lubricants at different temperatures and pressures. The temperature-dependent parameters of the equation of state have been calculated using corresponding state correlations, based on density at room temperature as scaling constants. It is shown that the knowledge of just liquid density at room temperature is sufficient to estimate the PVT properties of pure lubricants in different conditions. Therefore, there is no need to specify the potential energy curve, the experimental second virial coefficients, the critical constant, or some parameters like the Pitzer acentric factor and the heat of vaporization.

Also, the performance of the artificial neural network based on back propagation training for forecasting of the behavior of pure lubricants was investigated. The number of experimental data points set of density that are used in this study is 1269. The MLP is trained, validated, and tested with a random 70% (889 data points), 15% (190 data

**Table 6.** Comparison of the Calculated Density of ISM EOS, TM EOS and ANN with Literature in Various Temperatures and Pressures

Lubricant	NP*	$\Delta T(K)$	$\Delta P$ (bar)	AAD%	AAD%	AAD%
				(ISM)	(TM)	(ANN)
TEGDME	204	278.15-373.15	1-600	0.787	0.145	0.080
TriEGDME	204	278.15-373.15	1-600	0.968	0.121	0.120
PEC4	40	283.15-343.15	1.04-348.48	0.698	0.145	0.042
PEC5	99	278.15-353.15	1-450	0.569	0.269	0.073
PEC6	40	283.15-343.15	0.91-344.34	0.635	0.196	0.109
PEC7	99	278.15-353.15	1-450	0.987	0.350	0.099
PEC8	40	283.15-343.15	1.05-344.74	0.692	0.261	0.916
PEC9	88	283.15-353.15	1-450	0.968	0.421	0.185
PEB8	99	278.15-353.15	1-450	1.21	0.764	0.114
DMC	141	278.15-353.15	1-400	0.436	0.029	0.115
Squalane	143	278.15-398.15	1-600	0.693	0.440	0.095
DEGEE	72	283.15-353.15	1-250	0.387	0.034	0.075
Overall				0.75	0.26	0.16

points), and 15% (190 data points), respectively. Besides, “Tansig” and “Purelin” transfer functions are used in the hidden layer and output layer. Furthermore, the best network organization is explained via the back propagation algorithm of Levenberg-Marquardt (trainlm).

As stated, one of the important problems in the ANN is over-training. It can be overcome through appropriate selection of the number of neurons in the hidden layer. Training step should increase with increasing hidden neuron number; and an optimal number of hidden neurons lead to the best performance of the network in testing data phase. This trained network yields the best prediction on testing data and the use of more or less than the optimal number of hidden neurons was discouraged. The mean square error (MSE), average absolute deviation (AAD%) and correlation coefficient ( $R^2$ ) of training and testing data were selected as a measure of the net performance. As a result, the network

with one hidden layer (7 neurons) with grateful values of MSE, AAD and  $R^2$  of training and testing data presented the best prediction.

Finally, the average absolute deviations of the calculated molar densities of pure lubricants using the improved Ihm-Song-Mason equation of state (ISM EOS), Tao-Mason equation of state (TM EOS) and artificial neural network (ANN) at different temperatures and pressures were calculated; the overall average absolute deviation from the literature for 1269 data points were 0.75%, 0.25% and 0.17%, respectively (see Fig. 7).

## REFERENCES

- [1] Sethuramiah, A.; Kumar, R.; Chapter 2- Lubricants and Their Formulation, Modeling of Chemical Wear. Elsevier Press, 2016, p. 25-39.

- [2] Yousefi, F.; Karimi, H., Application of equation of state and artificial neural network to prediction of volumetric properties of polymer melts. *J. Ind. Eng. Chem.* **2013**, *19*, 498-507, DOI: 10.1016/j.jiec.2012.09.001.
- [3] Yousefi, F.; Karimi, H.; Gandomkar, Z., Equation of state and artificial neural network to predict the thermodynamic properties of pure and mixture of liquid alkali metals, *Fluid. Phase. Equilib.* **2014**, *370*, 43-49, DOI: 10.1007/s11581-011-0605-8.
- [4] Yousefi, F.; Karimi, A.; Alekisir, E.; Shishebor, M., Prediction of thermodynamic behavior of copolymers using equation of state and artificial neural network, *Colloid. Polym. Sci.* **2015**, *293*, 75-87, DOI: 10.1007/s00396-014-3391-9.
- [5] Zolfaghari, H.; Yousefi, F., Thermodynamic properties of lubricant/refrigerant mixtures using statistical mechanics and artificial intelligence. *Int. J. Refrig.* **2017**, *80*, 130-144, DOI: 10.1016/j.ijrefrig.2017.04.025.
- [6] Tao, F. M.; Mason, E. A., Statistical-mechanical equation of state for nonpolar fluids: Prediction of phase boundaries. *J. Chem. Phys.* **1994**, *100*, 9075-84.
- [7] Karimi, H.; Yousefi, F., Application of artificial neural network-genetic algorithm (ANN-GA) to correlation of density in nanofluids. *Fluid. Phase. Equilib.* **2012**, *336*, 79-83, DOI: 10.1016/j.fluid.2012.08.019.
- [8] Yousefi, F.; Moghadasi, J.; Papari, M. M.; Campo, A., Extension of tao-mason equation of state to mixtures: Results for PVTx properties of refrigerants fluid mixtures. *Ind. Eng. Chem. Res.* **2009**, *48*, 5079-84. DOI: abs/10.1063/1.466713.
- [9] Karimi, H.; Yousefi, F.; Papari, M. M., Extension of tao-mason equation of state to heavy n-alkanes. *Chin. J. Chem. Eng.* **2011**, *19*, 496-503, DOI: 10.1016/S1004-9541(13)60548-0.
- [10] Yousefi, F.; Karimi, H., P-V-T properties of polymer melts based on equation of state and neural network. *Eur. Polym. J.* **2012**, *48*, 1135-43, DOI: 10.1016/j.eurpolymj.2012.03.018.
- [11] Yousefi, F.; Karimi, H., Application of equation of state and artificial neural network to prediction of volumetric properties of polymer melts. *J. Ind. Eng. Chem.* **2013**, *19*, 498-507, DOI: 10.1016/j.jiec.2012.09.001.
- [12] McQuarrie, D. A., *Statistical Mechanics*. Harper and Row, New York, 1976, pp. 25-86.
- [13] Ihm, G.; Song, Y.; Mason, E. A., A New strong principle of corresponding states for nonpolar fluids. *J. Chem. Phys.* **1991**, *94*, 3839-3848, DOI: 10.1063/1.460684..
- [14] Weeks, J. D.; Chandler, D.; Anderson, H. C., Perturbation theory of the thermodynamic properties of simple liquids. *J. Chem. Phys.* **1971**, *54*, 5237-47, DOI: 10.1080/00268977200102111.
- [15] Song, Y.; Mason, E. A., Statistical-mechanical theory of a new analytical equation of state. *J. Chem. Phys.* **1989**, *91*, 7840-53, DOI: 10.1063/1.457252.
- [16] Carnahan, N. F.; Starling, K. E., Equation of State for Nonattracting Rigid Spheres. *J. Chem. Phys.* **1969**, *51*, 635-6, DOI: 10.1063/1.1672048.
- [17] Ihm, G.; Song, Y.; Mason, E. A., Strong principle of corresponding states: Reduction of a p-v-T surface to a line. *Fluid Phase Equilib.* **1992**, *75*, 117-25, DOI: 10.1016/0378-3812(92)87011-B.
- [18] Tsonopolous, C., Second virial coefficient of water pollution. *AIChE J.* **1978**, *24*, 1112-5, DOI: abs/10.1002/aic.690240625.
- [19] Eslami, H., Equation of state for nonpolar fluids: Prediction from boiling point constants. *Int. J. Thermophys.* **2000**, *21*, 1123-37, DOI: 10.1023/A:1013195118132.
- [20] Haykin, S., *Neural Networks: A Comprehensive Foundation*, 2nd ed. Prentice-Hall, New York, 1999; p. 101-150.
- [21] Xu, P.; Xu, S.; Yin, H., Application of self-organizing competitive neural network in fault diagnosis of suck rod pumping system. *J. Petrol. Sci. Eng.* **2007**, *58*, 43-8, DOI: 10.1016/j.petrol.2006.11.008.
- [22] Vaferi, B.; Rahnam, Y.; Darvishi, P.; Toorani, A. R.; Lashkarbolooki, M., Phase equilibria modeling of binary systems containing ethanol using optimal feedforward neural network. *J. Supercrit. Fluids.* **2013**, *84*, 80-8, DOI: 10.1016/j.supflu.2013.09.013.
- [23] Vaferi, B.; Karimi, M.; Azizi, M.; Esmaili, H., Comparison between the artificial neural network,

- SAFT and PRSV approach in obtaining the solubility of solid aromatic compounds in supercritical carbon dioxide. *J. Supercrit. Fluids*. **2013**, *77*, 45-51, DOI: 10.1016/j.supflu.2013.02.027.
- [24] Vafaei, B.; Eslamloueyan, R.; Ayatollahi, Sh., Simulation of steam distillation process using neural networks. *Chem. Eng. Res. Des.* **2009**, *87*, 997-1002, DOI: 10.1016/j.cherd.2009.02.006.
- [25] Bishop, C., *Neural Networks for Pattern Recognition*. Oxford: Oxford Clarendon, 1996, p. 114-145.
- [26] Ripley B., *Pattern Recognition and Neural Networks*. Cambridge: Cambridge University Press, 1996, p. 86-90
- [27] Comunas, M. J. P.; Baylaucq, A.; Boned, C.; Canet, X.; Fernandez, J., High-pressure volumetric behavior of x<sub>1</sub> 1,1,1,2-Tetrafluoroethane+(1-x)<sub>2</sub> 5,8,11,14-pentaoxapentadecane (TEGDME) mixtures. *J. Chem. Engng. Data*. **2002**, *47*, 233-8, DOI: 10.1021/je0155251.
- [28] Comunas, M. J. P.; Lopez, E. R.; Pires, P.; Garcia, J.; Fernandez, J., P-ρ-T measurements of polyethylene glycol dimethylethers between 278.15 and 328.15 K at pressures to 12 MPa. *Int. J. Thermophys.* **2000**, *21*, 831-51, DOI: 10.1023/A:1006606122944.
- [29] Comuñasa, M. J. P.; Fernández, J.; Baylaucq, A.; Canet, X.; Boned, C., P-ρ-Tx measurements for HFC-134a + triethylene glycol dimethylether system. *Fluid. Phase. Equilib.* **2002**, *199*, 315-34, DOI: 10.1021/je0101931.
- [30] Fedele, L.; Marinetti, S.; Bobbo, S.; Scattolini, M., PρT experimental measurements and data correlation of pentaerythritol esters. *J. Chem. Eng. Data*. **2007**, *52*, 108-15, DOI: pdf/10.1021/je060271a.
- [31] Fandino, O.; Garcia, J.; Comunas, M. J. P.; Lopez, E. R.; Fernandez, J., PρT measurements and equation of state (EoS) predictions of ester lubricants up to 45 MPa. *Ind. Eng. Chem. Res.* **2006**, *45*, 1172-82, DOI: abs/10.1021/ie050818z.
- [32] Fandino, O.; Pensado, A. S.; Lugo, L.; Lopez, E. R.; Fernandez, J., Volumetric behaviour of the environmentally compatible lubricants pentaerythritol-tetraheptanoate and pentaerythritol-tetrananoate at high pressures. *Green. Chem.* **2005**, *7*, 775-83(2005).
- [33] Fandino, O.; Pensado, A. S.; Lugo, L.; Comunas, M. J. P.; Fernandez, J., Compressed liquid densities of squalane and pentaerythritol-tetra-(2-ethylhexanoate). *J. Chem. Eng. Data*. **2005**, *50*, 939-46, DOI: abs/10.1021/je049580w.
- [34] Troncoso, J.; Bessieres, D.; Cerdeirina, C. A.; Carballo, E.; Romani, L., pρTx data for the dimethyl carbonate + decane system. *J. Chem. Engng. Data*. **2004**, *49*, 923-7, DOI: doi/abs/10.1021/je0342320.
- [35] Lugo, L.; Comuñas, M. J. P.; López, E. R.; Fernández, J., (p, V<sub>m</sub>, T, x) measurements of dimethylcarbonate + octane binary mixtures/I. Experimental results, isothermal compressibilities, isobaric expansivities and internal pressures. *Fluid. Phase. Equilib.* **2001**, *186*, 235-55, DOI:10.1016/S0378-3812(01)00518-0.
- [36] Fandino, O.; Pensado, A. S.; Lugo, L.; Comunas, M. J. P.; Fernandez, J., Compressed liquid densities of squalane and pentaerythritol-tetra-(2-ethylhexanoate). *J. Chem. Eng. Data*. **2005**, *50*, 939-46, DOI: abs/10.1021/je049580w.
- [37] Fandiño, O.; Lugo, L.; Comuñas, M. J. P.; López, E. R.; Fernández, J., Temperature and pressure dependences of volumetric properties of two poly(propylene glycol) dimethyl ether lubricants. *J. Chem. Thermodynamics*. **2010**, *42*, 84-9, DOI: 10.1016/j.jct.2009.07.013.
- [38] Lopez, E. R.; Lugo, L.; Comunas, M. J. P.; Garcia, J.; Fernandez, J., Liquid density measurements of diethylene glycol monoalkylethers as a function of temperature and pressure. *J. Chem. Eng. Data*. **2004**, *49*, 376-9, DOI: abs/10.1021/je034218n.